Available online at www.sciencedirect.com

ScienceDirect

Procedia Engineering 61 (2013) 276 – 283

Procedia Engineering

www.elsevier.com/locate/procedia

Parallel Computational Fluid Dynamics Conference (ParCFD2013)

Large-scale parallel computing for 3D gaseous detonation

Wang Cheng*, Bi Yong, Han Wenhu, Ning Jianguo

State Key Laboratory of Explosion Science and Technology, Beijing Institute of Technology
Beijing, China, 100081

Abstract

In numerical simulation of 3D gas detonation, due to the complexity of the computational domain in high resolution numerical computing negative density and pressure often emerge, which leads to blow-ups. In addition, a large number of grids resulting from relative mesh resolution and large-scale computing domain consume tremendous computing resources, which poses another challenge on the numerical simulation. In this paper, the positivity-preserving high order weighted essentially non-oscillatory (WENO) scheme is constructed without destroying the numerical accuracy and stability, and then the high-resolution parallel code is developed on the platform of Message Passing Interface (MPI). It is used to simulate the propagation of detonation wave in the 3D square duct with obstacles. The numerical results show that high-resolution parallel code can effectively simulate the propagation of 3D gas detonation wave in pipe, and the results also show that density and pressure are not negative in the event of diffraction. Therefore, the high-resolution parallel code provides an effective way to explore the new physical mechanism of 3D gas detonation.

Keywords: WENO scheme, positivity-preserving, parallel computing, detonation

1. Introduction

Detonation phenomenon is essentially three dimensional, thus some important structural characteristics can not be obtained from two-dimensional simulations. The numerical simulation of 3D detonation requires high grid resolution and algorithm, in particular for unstable detonation [1-4]. If the number of grid does not meet requirements, the front structure of detonation wave and the flow characteristics can not be captured, and the resulting law of detonation propagation wave does not reflect the real physical cases [5]. Furthermore, the 3D detonation wave requires a long computation time and sufficient length of the duct to form a self-sustaining detonation. If computational domain is very small, the boundary will affect the real detonation propagation characteristics. In numerical simulation, computational time and the number of grids occupy very large resource, which far exceeds computing capacity of a single CPU. Therefore, large parallel computing is a key to numerically investigate 3D detonation.

In practical detonation propagation, especially when detonation wave propagates in complex laneway, interaction of detonation wave with the boundaries and the resulting diffraction complicates the detonation propagation mechanism. In numerical simulation, pressure and density are often negative, which results in blow-ups. When density and pressure tend to be negative, they are forced to zero in the simple solution. However, this method damages the numerical accuracy and stability. To ensure pressure and density non-negative without destroying the accuracy and stability, the equations have to be resolved in high-resolution computing of 3D gas detonation.

First order and second order positivity-preserving schemes had already been studied in the reference by Linde [6,7]. Recently, Wang proposed a general framework for constructing arbitrarily high order positivity-preserving discontinuous Galerkin (DG) [8]. Zhang constructed high order positivity-preserving weighted essentially non-oscillatory (WENO) finite difference for 2D Euler equations [9]. However, to construct positivity-preserving high order finite difference WENO schemes for 3D, Euler equations have been seldom researched.

* Corresponding author. Tel.: +86-10-68914456
E-mail address: wangcheng@bit.edu.cn

Selection and peer-review under responsibility of the Hunan University and National Supercomputing Center in Changsha (NSCC)
doi:10.1016/j.proeng.2013.08.016

In this paper, we present an extension of 2D positivity-preserving method to construct positivity-preserving high order WENO finite difference schemes for 3D Euler equations with reaction source. And the positivity-preserving limiter is added to WENO finite difference scheme. Design of new limiter can not only preserve the positivity of pressure and density, but also maintain the conservation of conserved variables and high order accuracy of numerical solutions under suitable CFL condition. Based on this, we develop a high-resolution dynamic parallel code of 3D gaseous detonation. According to the computational domain, we dynamically adjust the computation of every process to ensure load balance. By applying the code to simulate the propagation of 3D detonation propagation in duct with obstacles, the numerical results agree well with the physical process.

2. Governing equations

Reactive-flow Euler equations with a source term are described by

$$\frac{\partial U}{\partial t}+\frac{\partial F(U)}{\partial x}+\frac{\partial G(U)}{\partial y}+\frac{\partial H(U)}{\partial z}=S$$

where, the conserved variable vector U, the flux vectors F, G and H as well as the source vector S are given , respectively, by

$$U=(\rho,\rho u,\rho v,\rho w,\rho E,\rho Y)^T$$
$$F=(\rho u,\rho u^2+p,\rho uv,\rho uw,(\rho E+p)u,\rho uY)^T$$
$$G=(\rho v,\rho uv,\rho v^2+p,\rho vw,(\rho E+p)v,\rho vY)^T$$
$$H=(\rho w,\rho uw,\rho vw,\rho w^2+p,(\rho E+p)w,\rho wY)^T$$
$$S=(0,0,0,0,0,\omega)^T$$
$$E=\frac{p}{(\gamma-1)}+\frac{1}{2}(u^2+v^2+w^2)+\rho qY$$
$$\omega=-K\rho Ye^{-(Ea/T)}$$
$$p=(\gamma-1)\rho e$$

where, p,ρ,E,T,u,v,w are pressure, density, total energy per unit volume, temperature and velocity, respectively; Y is reactant mass fraction, ω is reaction rate; γ is specific heat ratio, Ea is activation energy; K is pre-exponential factor; q is the heat of reaction; R is gas constant.

3. Positivity-preserving high order finite difference WENO schemes

Define the set of admissible states by $G=\{U\,|\,\rho>0,p\geq 0\}$, then G is a convex set, p is a concave function of U. We want to construct finite difference WENO schemes producing solutions in set G.

3.1 Positivity-preserving condition

For simplicity, we consider 1D Euler equations first,

$$U_t+f(U)_x=S \tag{1}$$

Let $A_{i+1/2}$ denote the Roe matrix[10] of the two states U^n_{i+1} and U^n_i, let $L_{i+1/2}$ and $R_{i+1/2}$ be the left and right eigenvector matrices of $A_{i+1/2}$ respectively, $\alpha=\max\left\|(|u|+c)\right\|$.

Let $f^{\pm}(U)=\frac{1}{2}\left[U\pm\frac{f(U)}{\alpha}\right]$ and $h_{\pm}=R_{\Delta x}(f^{\pm})$. Then we have the cell averages $\bar{h}^n_{\pm i}=f^{\pm}(U^n_i)$. Perform the WENO reconstruction to obtain $(h_+)^-_{i+\frac{1}{2}},(h_-)^+_{i+\frac{1}{2}}$.

Construct the flux by $\hat{f}_{i+\frac{1}{2}}=\alpha\left[(h_+)^-_{i+\frac{1}{2}}-(h_-)^+_{i+\frac{1}{2}}\right]$, let $\lambda=\frac{\Delta t}{\Delta x}$, then we get the finite difference scheme

$$U^{n+1}_i=U^n_i-\lambda\left(\hat{f}_{i+\frac{1}{2}}-\hat{f}_{i-\frac{1}{2}}\right)+\Delta tS(U^n_i,x_i)$$

$$= \frac{1}{2}U_i^n - \lambda\left(\hat{f}_{i+\frac{1}{2}} - \hat{f}_{i-\frac{1}{2}}\right) + \frac{1}{2}U_i^n + \Delta t S(U_i^n, x_i)$$

$$= \frac{1}{2}H^+ + \frac{1}{2}H^- + \frac{1}{2}\tilde{S} \tag{2}$$

where,

$$H^+ = \overline{h}_{+i}^n - 2\alpha\lambda\left[(h_+)^-_{i+\frac{1}{2}} - (h_+)^-_{i-\frac{1}{2}}\right] \tag{3}$$

$$H^- = \overline{h}_{-i}^n - 2\alpha\lambda\left[(h_-)^+_{i+\frac{1}{2}} - (h_-)^+_{i-\frac{1}{2}}\right] \tag{4}$$

$$\tilde{S} = U_{ijk}^n + 2\Delta t S(U_i^n, x_i) \tag{5}$$

Notice that (3) and (4) are finite volume schemes for h_+ and h_-. Obviously, if H^+, H^-, $\tilde{S} \in G$, then $U_i^{n+1} \in G$.

Let $q_i^+(x)$, $q_i^-(x)$ be the polynomials of degree k, such that $q_i^+(x_{i+\frac{1}{2}}) = (h_+)^-_{i+\frac{1}{2}}$, $q_i^-(x_{i-\frac{1}{2}}) = (h_-)^+_{i-\frac{1}{2}}$, the cell average of $q_i^{\pm}(x)$ is $\overline{h}_{\pm i}^n$.

Let $q_i^{+,*} = \dfrac{1}{1-\hat{w}_N}\sum_{k=1}^{N-1}\hat{w}_k q_i^+(\hat{x}_i^k)$, then

$$\overline{h}_{+i}^n = \frac{1}{\Delta x}\int_{I_i} q_i^+(x)\,\mathrm{d}x = \sum_{k=1}^{N}\hat{w}_k q_i^+(\hat{x}_i^k) = \sum_{k=1}^{N-1}\hat{w}_k q_i^+(\hat{x}_i^k) + \hat{w}_N(h_+)^-_{i+1/2} \tag{6}$$

Substituting (6) into (3), then (3) becomes

$$H^+ = (1-\hat{w}_N)q_i^{+,*} + (\hat{w}_N - 2\alpha\lambda)(h_+)^-_{i+1/2} + 2\alpha\lambda(h_+)^-_{i-1/2}$$

Therefore, if $q_i^{+,*}$, $(h_+)^-_{i+1/2}$, $(h_+)^-_{i-1/2} \in G$, $H^+ \in G$ under the CFL condition $2\alpha\lambda \le \hat{w}_N$.

Similarly, if $q_i^{-,*}$, $(h_-)^+_{i+1/2}$, $(h_-)^+_{i-1/2} \in G$, $H^- \in G$ under the CFL condition $2\alpha\lambda \le \hat{w}_N$, where $\hat{w}_1 = \hat{w}_N$. And $\tilde{S} \in G$ is discussed in [8].

From the above, the following theorem is obvious.

Theorem 1 Under the CFL condition $2\alpha\lambda \le \hat{w}_1$, if $q_i^{+,*}$, $(h_+)^-_{i+1/2}$, $(h_+)^-_{i-1/2}$, $q_i^{-,*}$, $(h_-)^+_{i+1/2}$, $(h_-)^+_{i-1/2} \in G$, the finite difference WENO scheme (2) will be positivity-preserving, i.e. $U_i^{n+1} \in G$.

Based on the above, finite difference WENO scheme for 3D Euler equations with source term is given by

$$U_{ijk}^{n+1} = U_{ijk}^n - \frac{\Delta t}{\Delta x}\left(\hat{f}_{i+\frac{1}{2},j,k} - \hat{f}_{i-\frac{1}{2},j,k}\right) - \frac{\Delta t}{\Delta y}\left(\hat{g}_{i,j+\frac{1}{2},k} - \hat{g}_{i,j-\frac{1}{2},k}\right) - \frac{\Delta t}{\Delta z}\left(\hat{h}_{i,j,k+\frac{1}{2}} - \hat{h}_{i,j,k-\frac{1}{2}}\right) + \Delta t S$$

Similarly, it can be written as

$$U_{ijk}^{n+1} = \frac{1}{4}\hat{F} + \frac{1}{4}\hat{G} + \frac{1}{4}\hat{H} + \frac{1}{4}\hat{S}$$

where

$$\hat{F} = U_{ijk}^n - 4\frac{\Delta t}{\Delta x}\left(\hat{f}_{i+\frac{1}{2},j,k} - \hat{f}_{i-\frac{1}{2},j,k}\right)$$

$$\hat{G} = U_{ijk}^n - 4\frac{\Delta t}{\Delta y}\left(\hat{g}_{i,j+\frac{1}{2},k} - \hat{g}_{i,j-\frac{1}{2},k}\right)$$

$$\hat{H} = U_{ijk}^n - 4\frac{\Delta t}{\Delta z}\left(\hat{h}_{i,j,k+\frac{1}{2}} - \hat{h}_{i,j,k-\frac{1}{2}}\right)$$

$$\hat{S} = U_{ijk}^n + 4\Delta t S$$

It is straightforward to extend the positivity-preserving results for 1D to 3D.

3.2 Positivity-preserving limiter

(1) At first, modify the density

Let $\overline{h} = (\overline{\rho}, \overline{\rho u}, \overline{\rho v}, \overline{\rho w}, \overline{\rho E}, \overline{\rho Y})^T$, for each cell I_i, modify the density

$$\hat{\rho}^{-}_{i+1/2} = \theta_i \hat{\rho}^{-}_{i+1/2} + (1-\theta_i)\overline{\rho}_i$$

where $\theta_i = \min\left\{1, \left|\frac{\overline{\rho}_i - \varepsilon}{\overline{\rho}_i - \rho_{\min}}\right|\right\}$, ε is a small number. In practice, we can choose $\varepsilon = 10^{-13}$.

(2) Then, modify the pressure

Define

$$\hat{u}^{-}_{i+1/2} = \left(\hat{\rho}^{-}_{i+1/2}, \hat{\rho}u^{-}_{i+1/2}, \hat{\rho}v^{-}_{i+1/2}, \hat{\rho}w^{-}_{i+1/2}, E^{-}_{i+1/2}, \rho Y^{-}_{i-1/2}\right)^T$$

Let

$$\tilde{u}^{-}_{i+1/2} = \theta_i[\hat{u}^{-}_{i+1/2} - \overline{u}_i] + \overline{u}_i$$

Such that

$$p(\theta_k[\hat{u}^{-}_{i+1/2} - \overline{u}_i] + \overline{u}_i) \geq 0 .$$

For each x, find θ_x as solution of

$$p(\theta_x[\hat{w}^{-}_{i-1/2} - \overline{w}_i] + \overline{w}_i) = 0 .$$

4. Realization of high-resolution parallel program

Computational domain is divided into N sub-domains, and every sub-domain is undertaken by a process. Message communication of the interface between sub-domains is completed by library function of MPI. For example, 5-th order WENO scheme requires three layers of ghost grid outside boundary, and message communication takes lots of time. Therefore, non-blocking communication MPI_ISEND (buf,count,datatype,dest,comm,req) is used for data transmission between sub-domain interfaces, where req denotes status and is used to check the status of message transmission. It is not necessary to return after finishing data transmission. So, overlapping of communication and computing improves the efficiency of program execution [11].

Basic idea of high-resolution parallel steps:

(1) Define array A(nx(t),ny(t),nz(t)) for 3D domain, where t is time. Thus sub-domain arrays are Asub(nx(t)/cut_x, ny(t)/cut_y, nz(t)/cut_z)= Asub(nx, ny, nz), where cut_x, cut_y and cut_z are the number of divisions in x, y and z directions , respectively. Assume cut_x=4, cut_y=4 and cut_z=4, the sub-domain is shown in Fig.1.

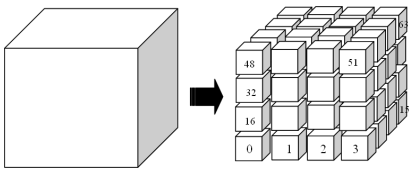

Fig.1 Three-dimensional cutting of the computational domain

(2) Expand sub-domain arrays Asub(-md:nxm, -md:nym, -md:nzm), where md=3, nxm=nx+md, nym=ny+md, nzm=nz+md.

(3) Number the divided sub-domain

Call library function MPI_Comm_rank(MPI_COMM_WORLD, mpirank, ierr) to achieve numbering sub-domain integer, mpirank is the index of number order, from 0 to cut_x*cut_y* cut_z-1.

(4) The data structure of the communication

Define one-dimensional array send_bufx1(n), send_bufx2(n), and put x-direction variables into send_bufx1(n)， send_bufx2(n), where n is total number. Similarly, put y, z-direction variables into send_bufy1(n), send_bufy2(n) and send_bufz1(n), send_bufz2(n) in order.

(5) Data communication between sub-domain interfaces

Fig.2 shows the message transmission in x-direction. Domain 0 sends message in send_bufx1(n)， send_bufx2(n) to domain 1 and 3, meanwhile receiving message from domain 1 and 3. Similarly, communication object of domain 3 is domain 0 and 2.

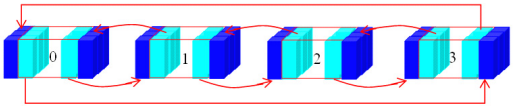

Fig.2 Sketch of message communication among sub-domains

5. Numerical simulation of 3D detonation

5.1 Detonation diffraction

To verify the positivity-preserving method, we simulate the diffraction behaviour when the 3D detonation propagates from the duct to a free space. The width and height of duct are 5 and 3, respectively. An ignition zone is set on the left of the duct, while the remaining region is filled with un-reacted mixture. The left of the duct is in flow condition, and other boundaries are walls.

Fig.3 shows the pressure and density contour at some time when detonation propagates into free space. As can be seen from Fig.3, a region of low pressure and density can be seen obviously. Minimum value of density and pressure is very small, but the values of pressure and density in this region are not negative. This fully demonstrates that reliance of the positivity-preserving method is very good.

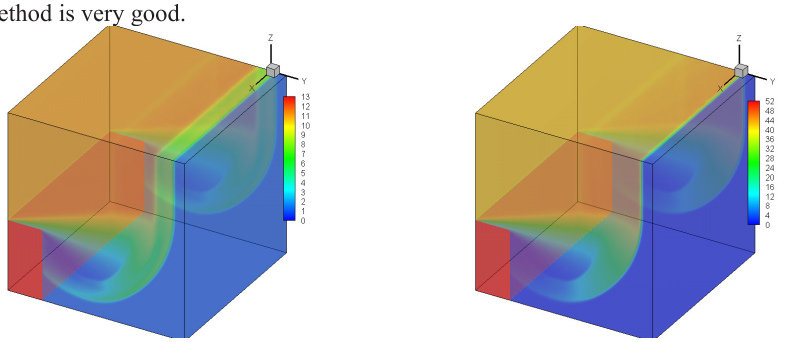

(a) Density (b) Pressure

Fig.3 Colored contour of density and pressure

5.2 Effect of obstacles on detonation propagation

Take 3D square duct as computing domain. Its length and width are 126 and 16, respectively. The width of obstacles is 0.6. The heights of obstacles (H) are 2.0, 4.0 and 6.0, respectively. The space of obstacles is 16. The one-dimensional ZND analytical solution is used as initial value. The left of the duct is inflow boundary, and the other is rigid walls[12].

(1) One obstacle

Fig.4 shows the propagation of detonation wave in case of one obstacle. It can be seen from Fig.4(a) that a very low pressure rarefaction zone emerges before the obstacle due to diffracting when detonation wave passes the obstacle. As shown in Fig.4(b), we can observe that the wave passes the obstacle, with pressure on its front decreasing, then is reflected by the walls. The local detonation is formed and the triple-point structure can be seen obviously [13].

Fig.5 shows maximum pressure history on the walls when the obstacle heights are 2.0 and 4.0, respectively. It can be seen that when the obstacle height is 2.0, re-ignition occurs. Cellular detonation can be formed and irregular cells appear on the walls. When the height reaches 4.0, re-ignition can also occur after passing the obstacle[14], as shown in Fig. 5(b).

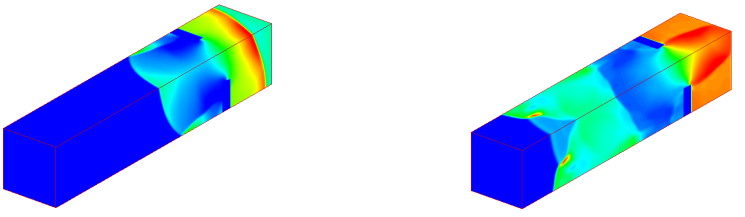

(a) t= 1.34 (b) t= 5.82

Fig.4 Propagation of detonation wave in case of one obstacle: (A fourth part of total domain along axis line)

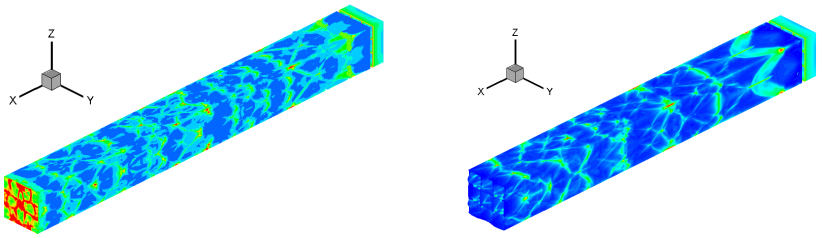

(a) H=2.0 (b) H=4.0

Fig.5 Maximum pressure history on the walls in case of one obstacle

(2) Two obstacles

Fig.6 shows the propagation of detonation wave in case of two obstacles of H=2.0. It can be seen that at t=1.20, the wave front takes on a spherical characteristics and diffracting wave front collides with the walls and reflection occurs. Thus transverse waves appear on every wall. At t=1.88, transverse waves on the neighboring walls collide each other at wall corner and strong local explosions happen. The resulting energy ignites the un-reacted gas near the corner and gives impetus to the front of local detonation. At t=2.06, the front collides with the second obstacle and rectangular structure is formed. The front contains two pairs of triple-point lines, one of which are parallel to the y-direction and the other parallel to the z-direction. Each pair of the triple-point lines moves in opposite direction parallel to the front. At t=2.85-4.05, the triple-point lines collide at the axis line of the duct and separate each other. Then the triple-point lines split and the number of triple points on every wall increases.

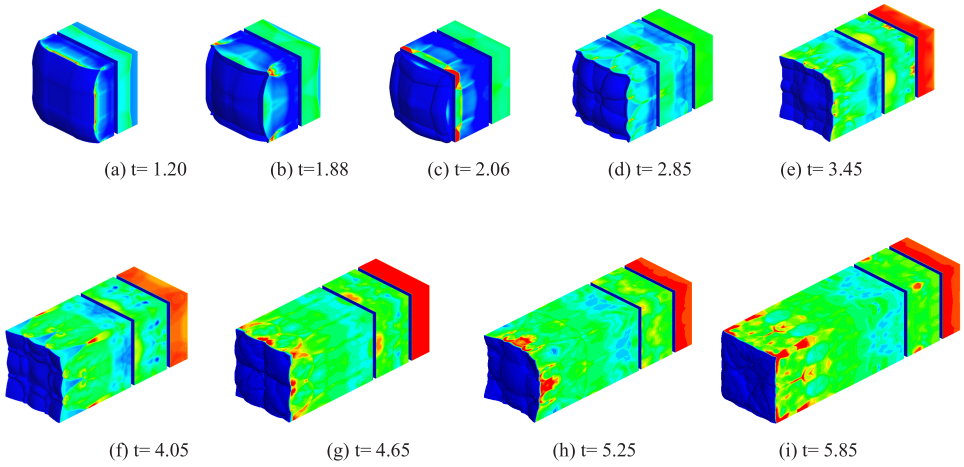

(a) t= 1.20 (b) t=1.88 (c) t= 2.06 (d) t= 2.85 (e) t= 3.45

(f) t= 4.05 (g) t= 4.65 (h) t= 5.25 (i) t= 5.85

Fig.6 Propagation of detonation wave in case of two obstacles of H=2.0

However, the front still maintains rectangular structure. At t=4.65-5.85, due to instability of detonation the triple-point lines become irregular and detonation cells become irregular too, as shown in Fig. 7(a).

Fig.7 shows maximum pressure history on the walls at different obstacles height. It can be observed that when obstacles height is 2.0, re-ignition behavior can occur. After a low velocity stage, cellular detonation can be formed and irregular cells appear on the walls. It can be seen further that after passing the second obstacle, detonation initially propagates in rectangular mode and slapping waves appear on the walls. Then the mode of detonation transits from the rectangular to the diagonal and slapping waves on the walls disappear. Over time, detonation cell splits and its size becomes smaller, as shown in Fig.7(a). As the height of the obstacles increases, detonation attenuates. At H=4.0, most of energy is consumed between the two obstacles. The result is that re-ignition behavior can not occur after passing the obstacle. At H=6.0, maximum pressure in the walls has become very weak and detonation quenches after passing the second obstacle, as shown in Fig. 7(c). Hence, as the height of obstacles increases, propagation of detonation wave can be effectively inhibited.

Fig.8 shows the propagation of detonation wave at different obstacles height. When obstacle height is 2.0, local re-ignition behavior occurs and local detonation is formed. The triple-point structure on the front can be seen clearly. As the height of obstacles increases, detonation attenuates. It can be seen that a low pressure zone among obstacles becomes larger as the height increases. When the height reaches 6.0, nearly all energy is blocked by the obstacles and the wave has become very weak after passing the second obstacle, as shown in Fig.8(c). The conclusion is consistent with [15, 16].

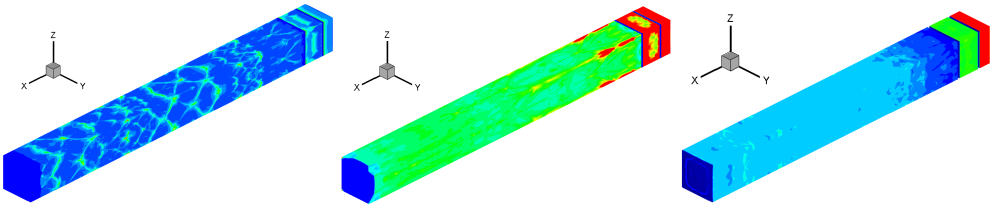

(a) H=2.0 (b) H=4.0 (c) H=6.0

Fig.7 Maximum pressure history on the walls at different obstacle heights

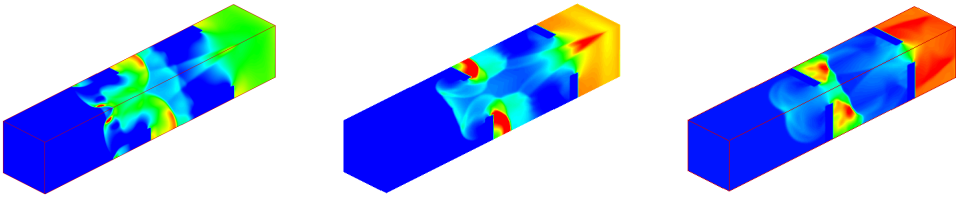

(a) t= 2.87 (b) t= 2.84 (c) t= 3.25

Fig.8 Propagation of detonation wave at different obstacle heights: (A fourth part of total domain along axis line)

6. Conclusions

A 3D detonation MPI parallel code is developed to investigate the effect of obstacles on the detonation wave based on positivity-preserving high order finite difference WENO schemes. The numerical results show that high-resolution parallel code can effectively simulate the propagation of 3D gas detonation in large-scale tube with obstacles. It can be found that pressure and density are positive. Numerical results also show that when detonation wave diffracts through obstacles, the propagation of detonation wave can be inhibited by increasing the number of obstacles. As the height of obstacles increases, detonation wave becomes weaker and weaker after passing two obstacles. Additionally, high-resolution parallel code saves communication time of data in interface, and further enhances the computational efficiency. It not only improves the computational efficiency but also the resolution of the detonation wave front. Therefore, it is a means to explore new physical mechanism of 3D gaseous detonation.

Acknowledgements

This research is supported by the National Natural Science Foundation of China under grants 11221202 and 11272056, National Basic Research Program of China (Grant Nos. 2010CB832706 and 2011CB706904), and the Foundation of State Key Laboratory of Explosion Science and Technology (Grant No. ZDKT11-01).

References

[1] Sharpe G. J., 2001. The effect of curvature on detonation waves in Type Ia supernovae. Monthly Notices of the Royal Astronomical Society 322, p. 614.
[2] Hwang P., Fedkiw R. P., Merriman B., Aslam T.D., Karagozian A.R., Osher S.J., 2000, Numerical resolution of pulsating detonation waves[J]. Combustion Theory and Modelling 4, p.217.
[3] Wang G., Zhang D.L., Liu K.X., Wang J.T., 2008, An improved two-dimensional CE/ SE method and its high order schemes. Chinese Journal of Computational Mechanics, 25, p. 741.
[4] Zai J.M., Wang S.H., Li Y.C., Yang J.M., 2010. Numerical simulation of primary-secondary shock wave propagation in duct with waring cross-section. Chinese Journal of Computational Mechanics, 27, p. 925.

[5] Tsuboi N., Asahara M., Eto K., Hayashi AK., 2008. Numerical simulation of spinning detonation in square duct. Shock Waves, 18, p. 329.
[6] Einfeldt B., Munz C.D., Roe P.L., Sjogreen B., 1991. On Godunov-type methods near low densities. Journal of Computational Physics, 92, p. 273.
[7] Linde T., Roe P.L., Robust Euler codes, Thirteenth Computational Fluid Dynamics Conference, AIAA Paper-97, p. 2098.
[8] Wang C., Zhang X.X., Shu C.W., Ning J.G., 2012. Robust high order discontinuous Galerkin schemes for two-dimensional gaseous detonations, Journal of Computational Physics, 231, p. 653.
[9] Zhang X.X., Shu C.W., 2012. Positivity-preserving high order finite difference WENO schemes for compressible Euler equations. Journal of Computational Physics, 231, p. 2245.
[10] Roe P.L., 1997. Approximate Riemann solvers, parameter vectors, and difference schemes, Journal of Computational Physics, 135, p. 250.
[11] Dou Z.H., 2001. High performance computing Parallel programming. Beijing: Tsinghua University Press.
[12] Knystautas R., Lee J.H., Guirao C.M., 1982. The critical tube diameter for detonation failure in hydrocarbon-air mixtures. Combustion and Flame, 48, p. 63.
[13] Pintgen F., Shepherd J.E., 2009. Detonation diffraction in gases. Combustion and Flame, 156, p. 665.
[14] Xu B.P., Wen J.X., Tam V.H.Y., 2010. The effect of an obstacle plate on the spontaneous ignition in pressurized hydrogen release: A numerical study. International Journal of Hydrogen Energy, 36, p. 2637.
[15] Valiev D., Bychkov V., Akkerman V., Law C.K., Eriksson L.E. 2010. Flame Acceleration in Channels with Obstacles in the Deflagration-to-detonation Transition. Combust Flame 57, p. 1012.
[16] Pantow E.G., Fischer M., Kratzel T., 1996. Decoupleing and recoupling of detonation waves associated with sudden expansion. Shock Waves, 6, p. 131.